

International Institute for Carbon-Neutral Energy Research



Processing yttrium-doped barium zirconate cerate for energy-efficient electrochemical devices

K. Leonard¹, M. E. Ivanova², W. A.
Meulenberg², T. Ishiraha¹, and H. Matsumoto¹

¹*Advanced Energy Conversion Systems (WPI-I²CNER, Kyushu University)*

²*IEK-1 Forschungszentrum Jülich GmbH, Germany*



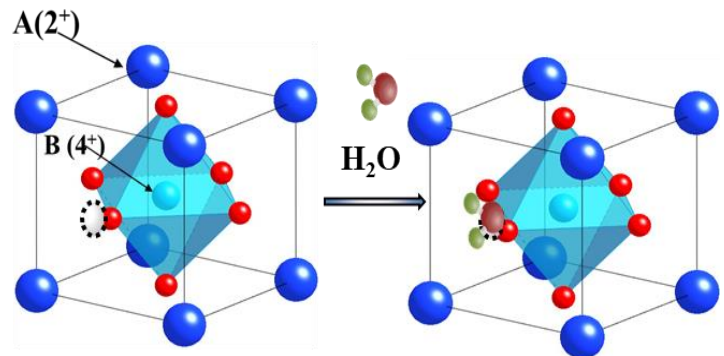
6th International Workshop
PROSPECTS ON PROTONIC CERAMIC CELLS
June 8 -10, 2022 - Dijon, France



KYUSHU UNIVERSITY



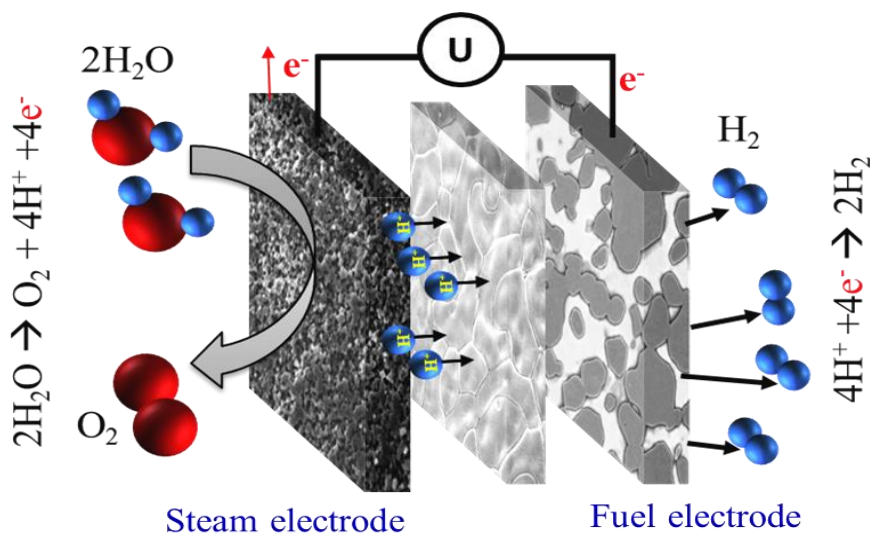
General Introduction



Ceramic material that exhibits proton conductivity in the temperature range 400 ~ 800 °C

Useful for energy conversion and storage.

- ✓ Efficient production of electric power (PCFC)
- ✓ Efficient production of valuable fuels, (PCEC)



Key indicators for electrolysis performance evaluation

Operating voltage

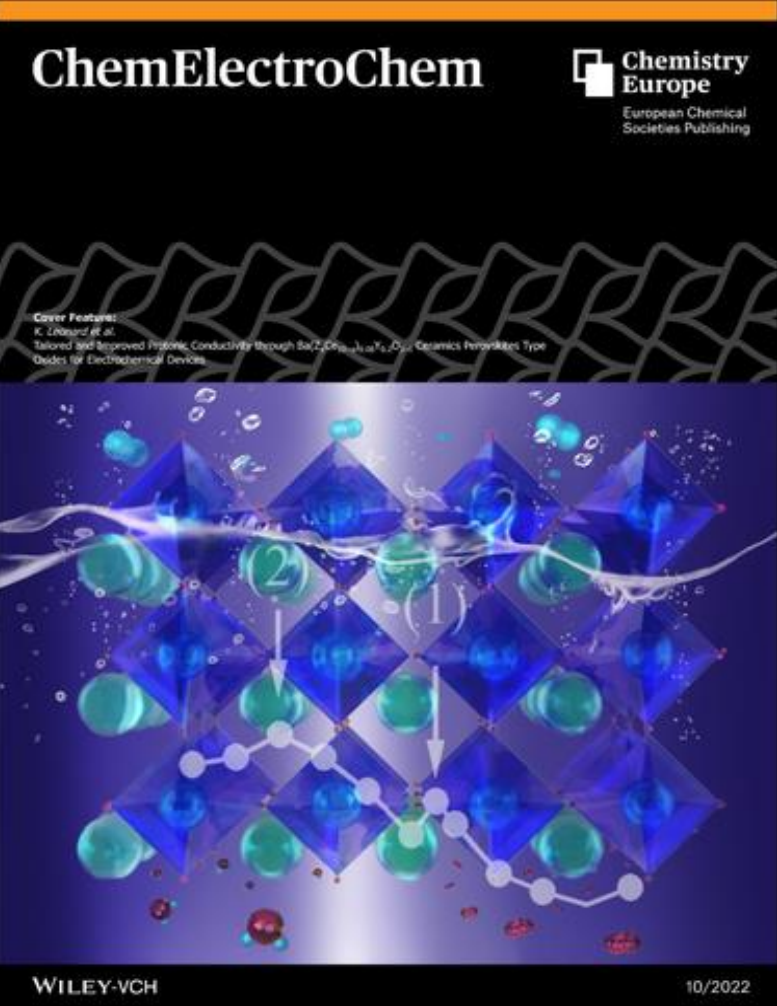
- ✓ defines the electrolysis (electrical) efficiency.

Current density

- ✓ determines hydrogen production per cell area

Operating voltage
↓ Low

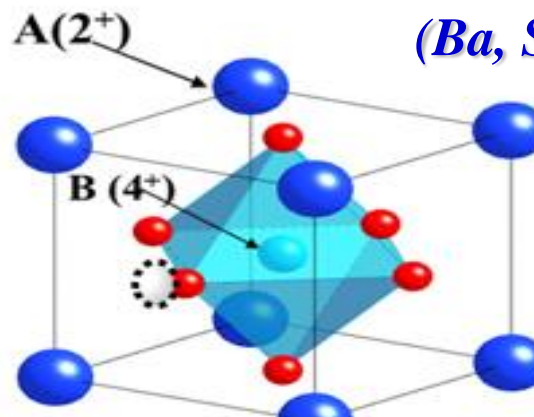
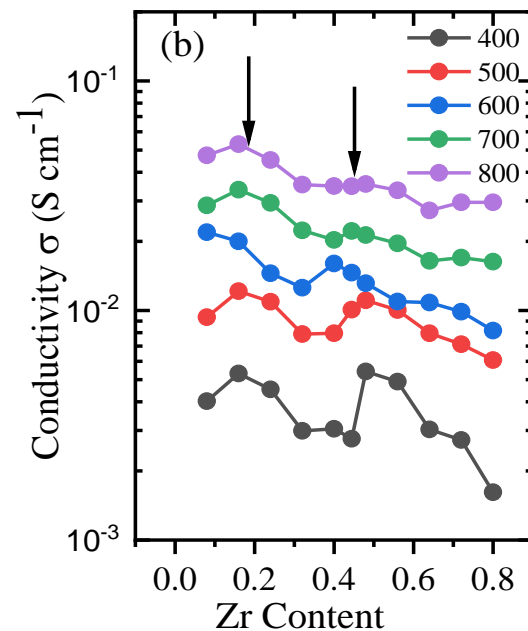
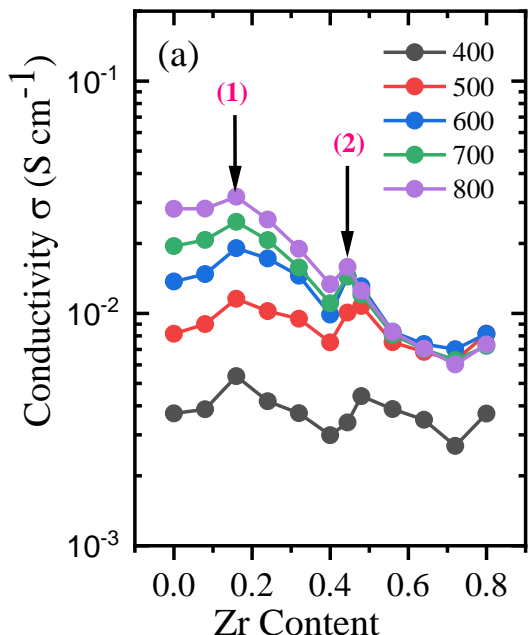
Current density
↑ High



K. Leonard et al. *ChemElectroChem* (2022), 9

$\text{BaZr}_{0.44}\text{Ce}_{0.36}\text{Y}_{0.2}\text{O}_{3-\delta}$ (1) demonstrates a superior ionic conductivity to stability trade-off (10.1 mS/cm @ 500°C) $\text{BaZr}_{0.16}\text{Ce}_{0.64}\text{Y}_{0.2}\text{O}_{3-\delta}$ (2) superior σ_H 11.5 mS/cm

State-of-the-art electrolytes-($\text{Ba},\text{Sr})(\text{Ce},\text{Zr},\text{Y})\text{O}_{3-\delta}$

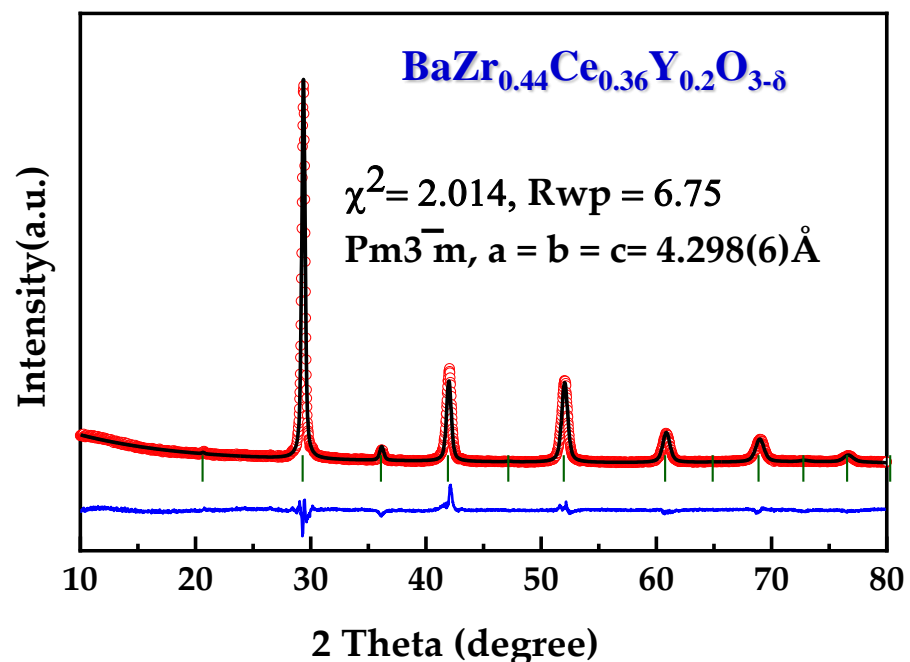


$(\text{Ba}, \text{Sr})(\text{Ce}, \text{Zr}, \text{Y})\text{O}_{3-\delta}$

perovskite B-site.
 $\text{Zr:Ce}=5/4$

Two new composition variants

Phase and structural characterization



900 °C perovskite dominant phase, however with some secondary phases (BaCO₃, CeO₂, Y₂O₃)
1300 °C single-phase perovskite structures

BaZr_{0.44}Ce_{0.36}Y_{0.2}O_{3-δ} (1)

Space group

Pm $\bar{3}m$

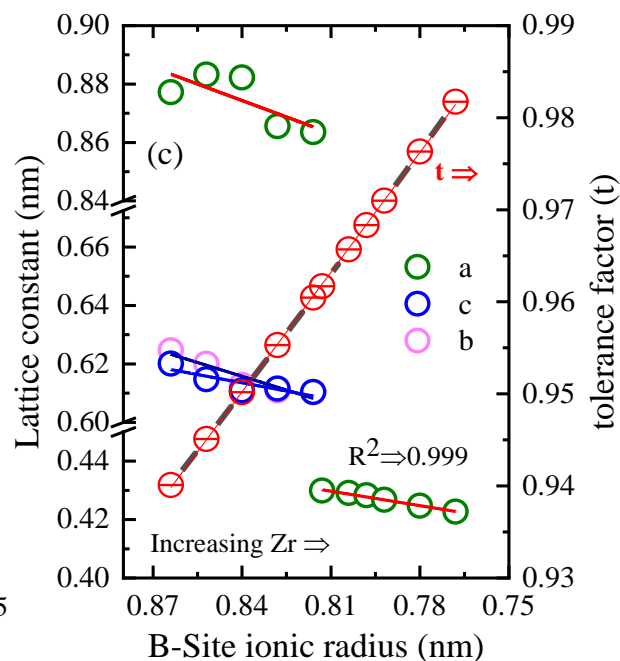
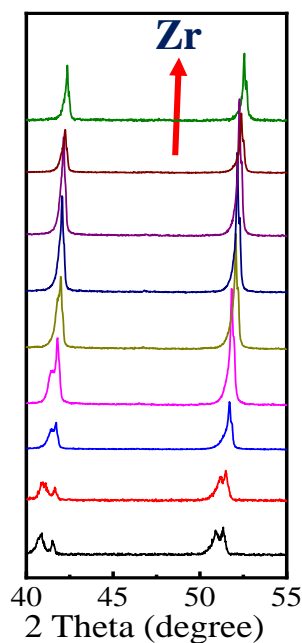
BaZr_{0.16}Ce_{0.64}Y_{0.2}O_{3-δ} (2)

Lattice parameter

$a = 4.2986$

$a = 8.8328$, $b = 6.2678$
 $c = 6.1475$

Ba(Zr_xCe_{10-x})_{0.08}Y_{0.2}O_{3-δ} ($1 \leq x \leq 9$)



The range $5.5 \leq x \leq 9$ =cubic perovskites

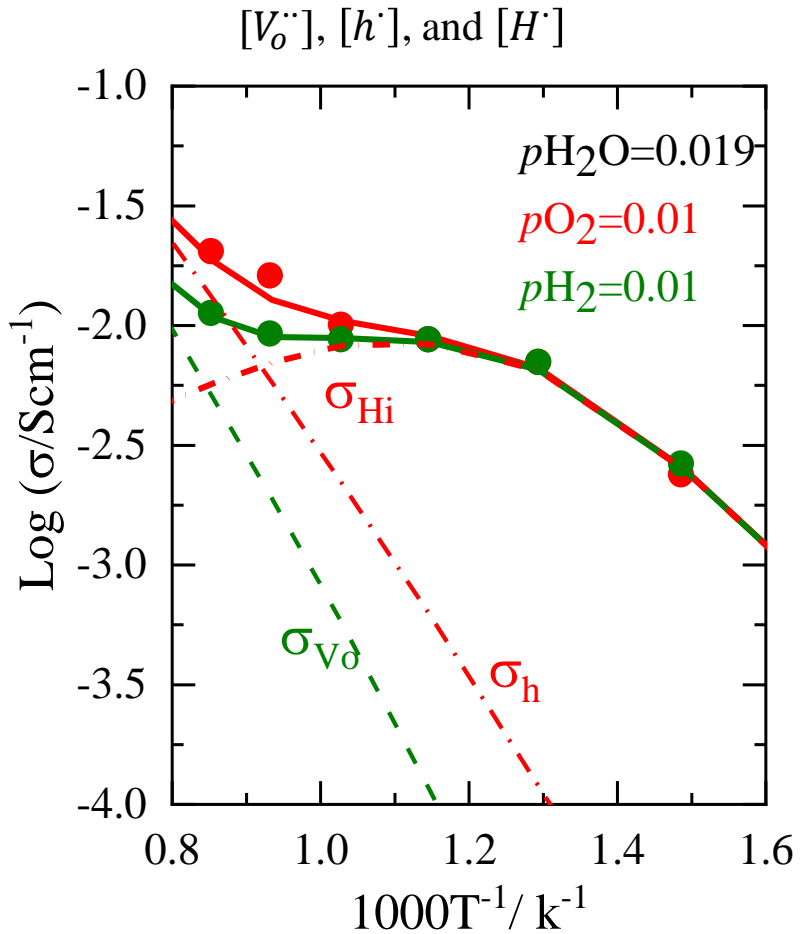
The range $1 \leq x \leq 5$ =orthorhombic

- ✓ An angular shift of the XRD pattern towards higher angles reflecting the substitution of Ce⁴⁺ for the Zr⁴⁺ in the lattice
- ✓ Linear dependence of the calculated lattice constants against the B-site ionic radius

Protonic electrolyte development

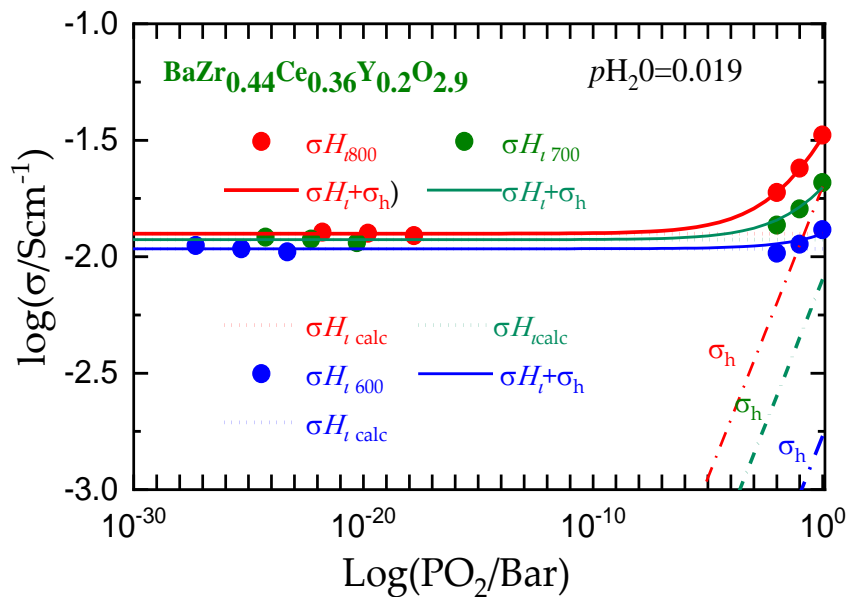
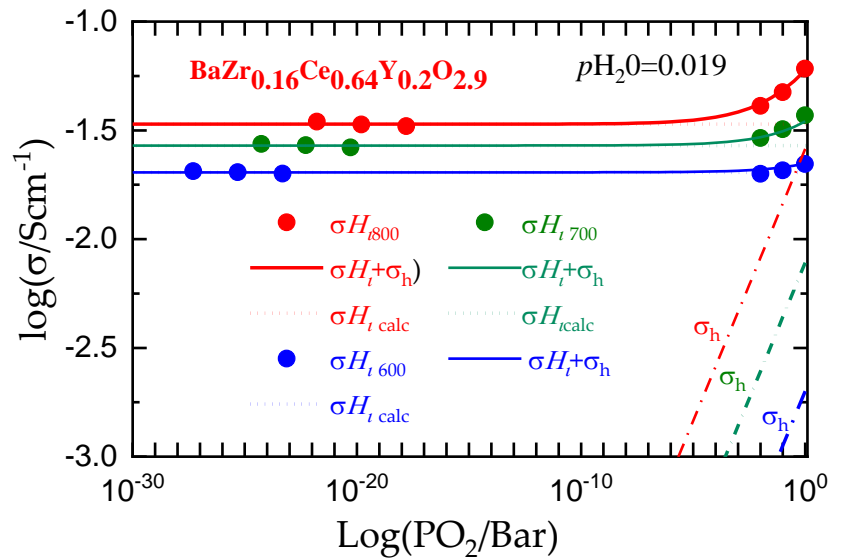
$BaZr_{0.44}Ce_{0.36}Y_{0.2}O_{2.9}$ (BZCY(54)_{8/9}2)

Many charge carriers existing simultaneously

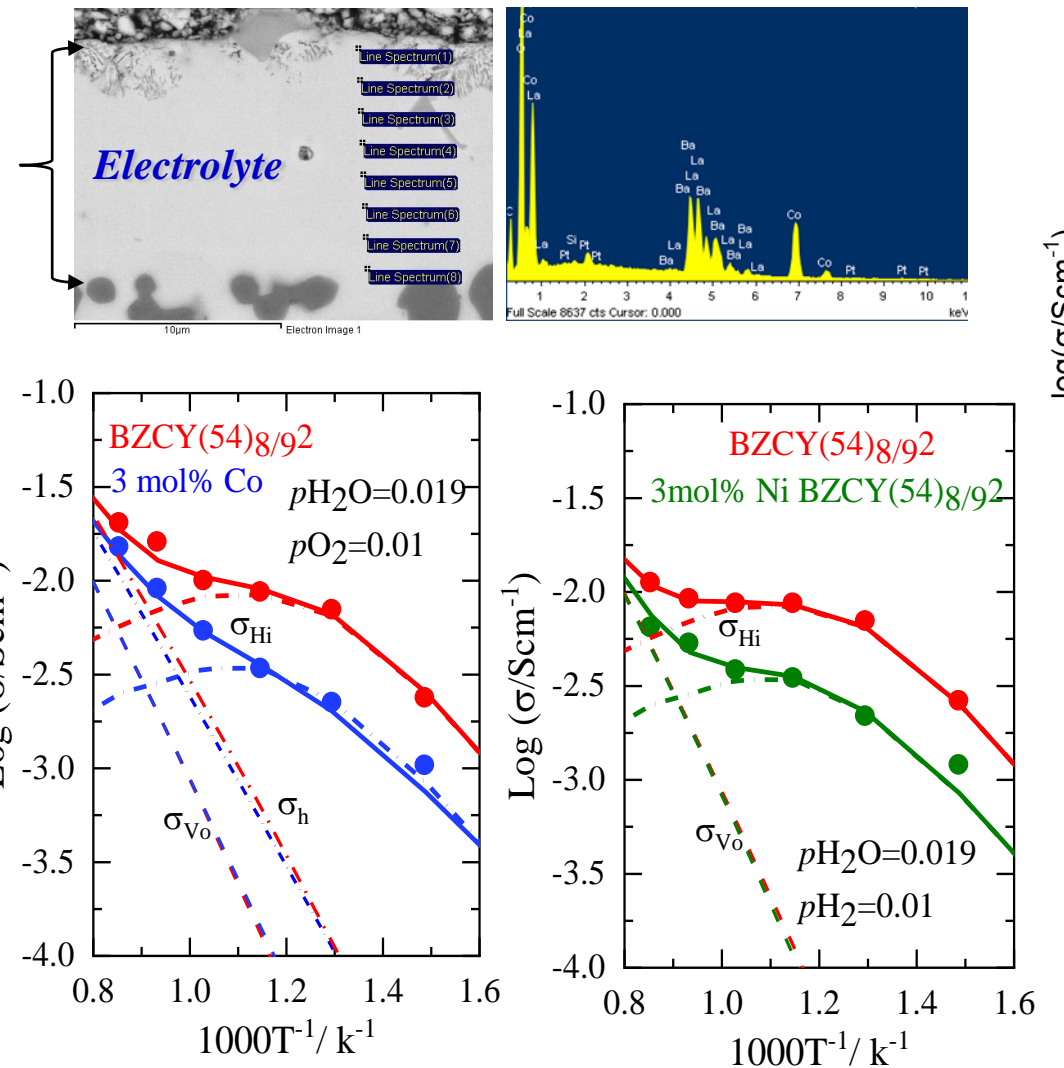


- The hole conductivity is minimal at 600 °C
- The hole conductivity increases at 800 °C in oxidizing atmosphere

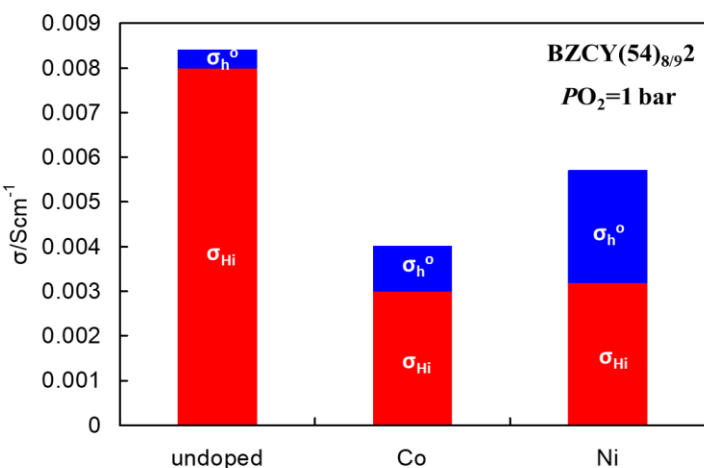
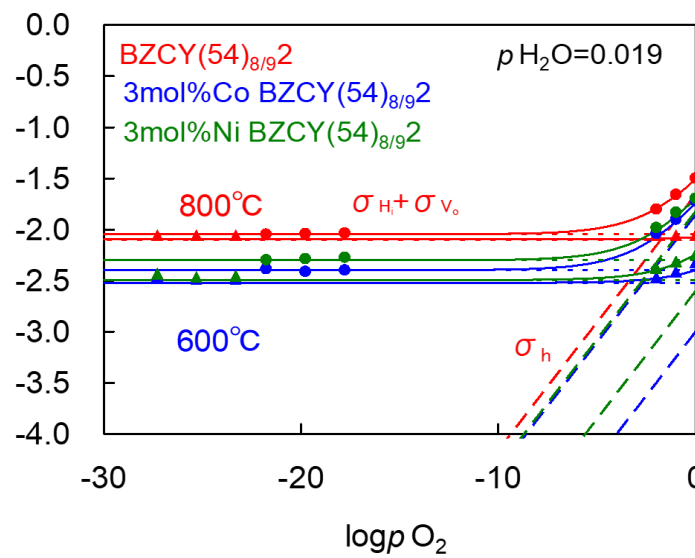
$P(O_2)$ dependence of conductivity



Effect of Co and Ni addition to $\text{BaZr}_{0.44}\text{Ce}_{0.36}\text{Y}_{0.2}\text{O}_{2.9}$



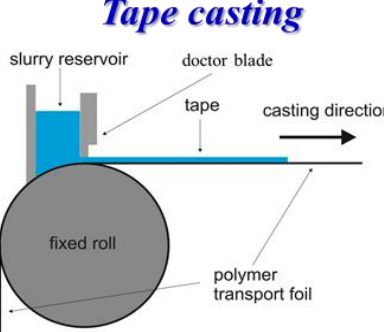
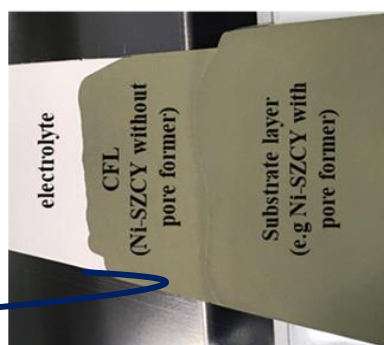
$P(\text{O}_2)$ dependence of conductivity



An ~1/3 drop in Conductivity by either Ni and Co addition

Achievements and progress

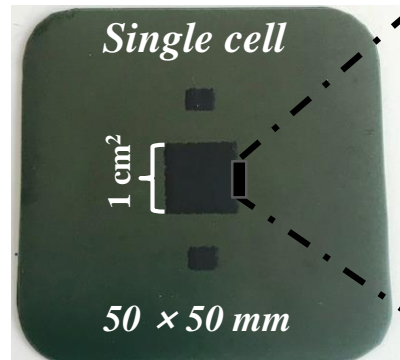
Improved Processing and fabrication by Sequential tape casting

<i>Electrolyte</i>	<i>Cathode (functional layer)</i>	<i>Cathode (substrate)</i>	<i>Anode</i>
(12~20 μ m) $BaZr_{0.44}Ce_{0.36}Y_{0.2}O_{2.9}$	(8~15 μ m) NiO- $BaZr_{0.44}Ce_{0.36}Y_{0.2}O_{2.9}$	(~ 0.4 mm) NiO- $BaZr_{0.44}Ce_{0.36}Y_{0.2}O_{2.9}$	(~25 μ m) $Ba_{0.5}La_{0.5}CoO_{3-\delta}$
Tape casting 			Screen printing 

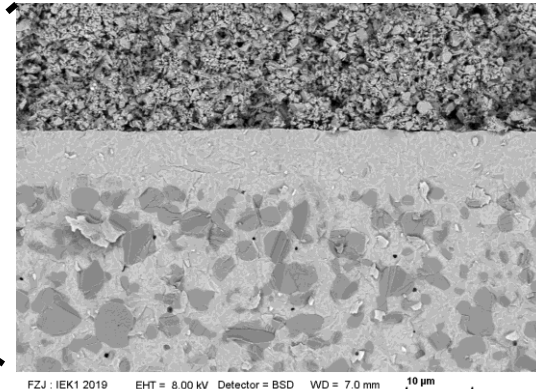
Punching, cutting and Lamination



De-binding and Sintering

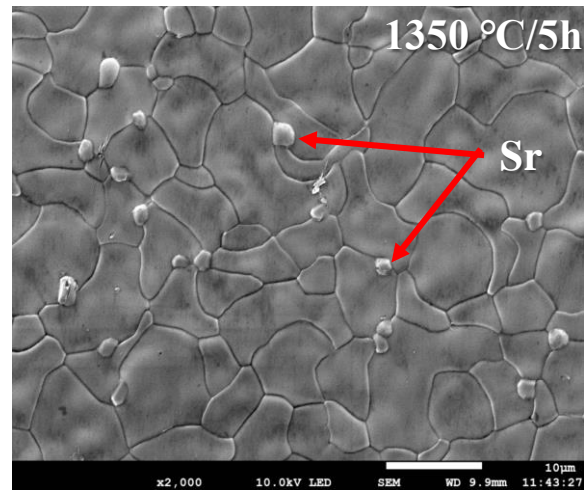
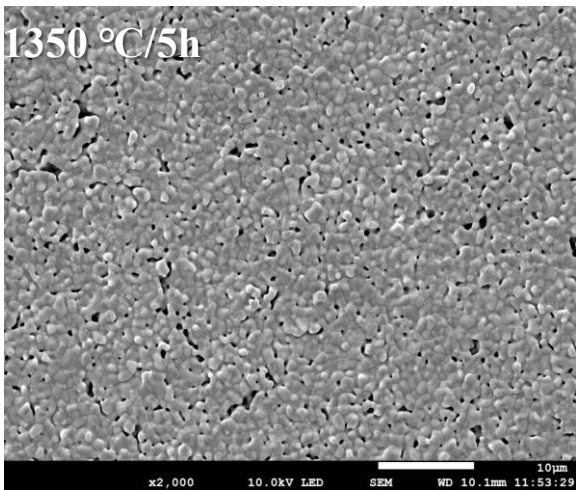
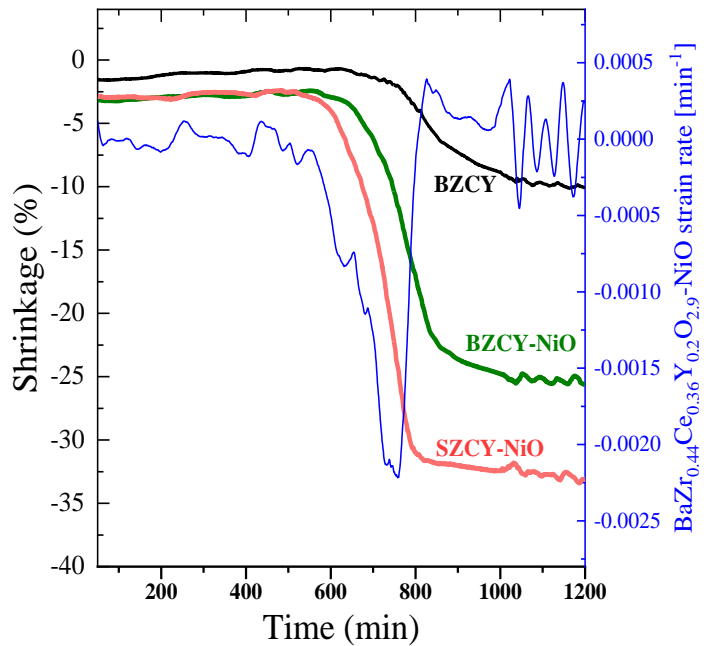


Cell Microstructure



Enhanced sinter-ability with $\text{NiO-SrZr}_{0.5}\text{Ce}_{0.4}\text{Y}_{0.1}\text{O}_{3-\delta}$

Lowering the sintering temperature of the $\text{BaZr}_{1-x-y}\text{Ce}_x\text{Y}_y\text{O}_{3-\delta}$ (BZCY) based half-cell below 1300°C is our utmost desire.



Liquid phase sintering

BaO-NiO



SrO-NiO



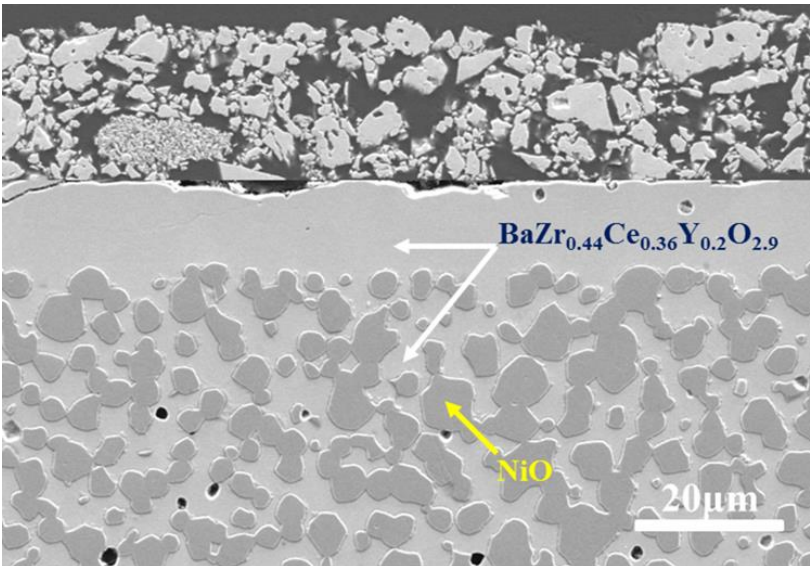
Lower Temp.

Higher temp.

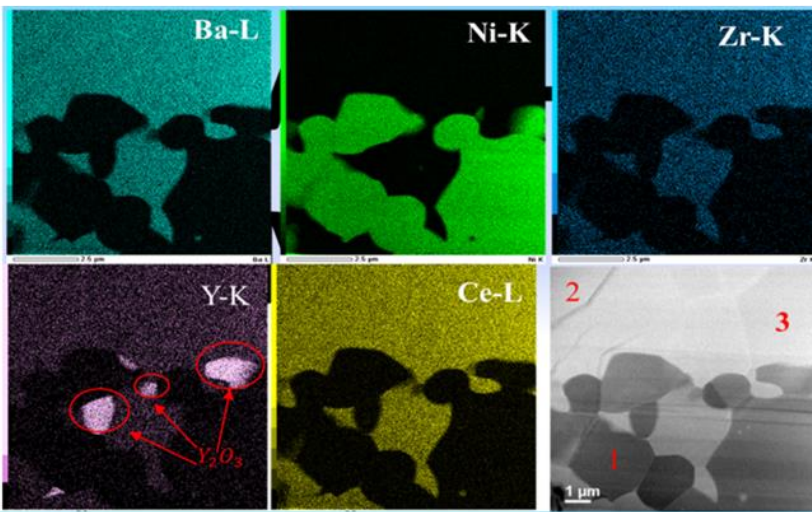
✓ *$\text{NiO-SrZr}_{0.5}\text{Ce}_{0.4}\text{Y}_{0.1}\text{O}_{3-\delta}$ substrate positively influenced the densification of BZCY(54)_{8/9}2*

✓ *Lowering operating temperature reduces nickel mobility and nucleation, reducing the driving force of this degradation*

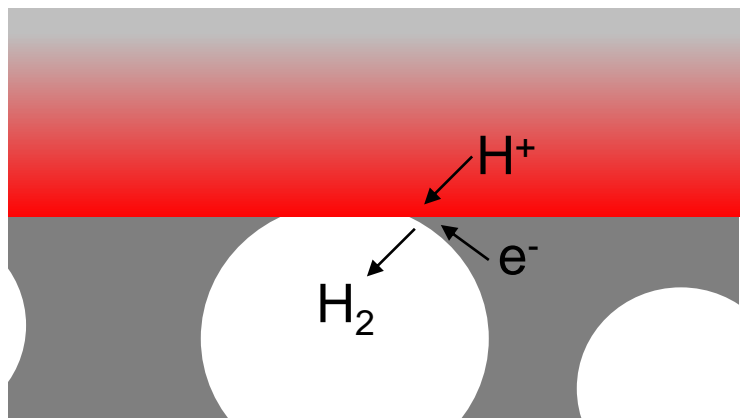
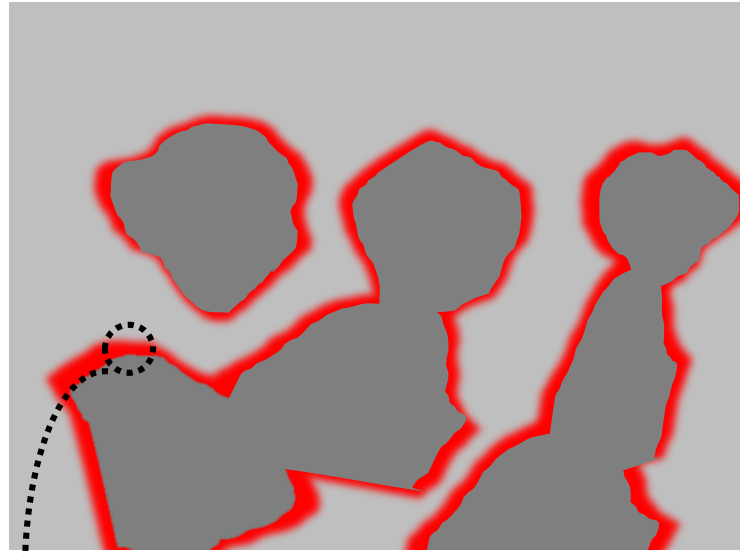
Schematic of Ni diffusion



BZCY / Ni-BZCY sintered at 1500 °C



- **Ba loss by evaporation, leading to Y_{Ba^*}**



➤ Ni diffuse to the electrolyte in the vicinity of NiO grain, resulting in an increase of resistance. High resistance part is in series with the electrode reaction

Progress on bottom size cell configuration (PCEC mode)

BLC| BZCY| Ni-SZCY541

Cell size: $\phi 22$ mm, Anode Size: $\phi 8$ mm

Electrolyte thickness: $\sim 12 \mu\text{m}$

Anode gas: 1% O_2 -Ar, 20 % H_2O

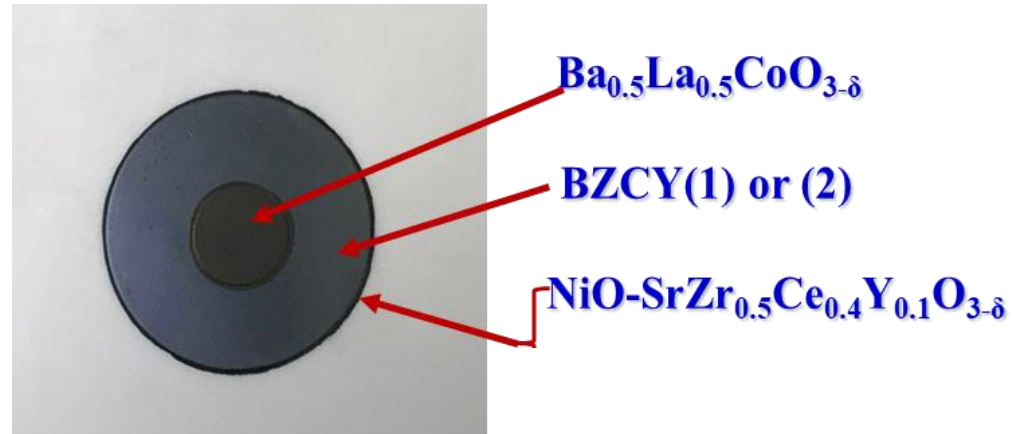
Cathode gas: 1% H_2 -Ar, 2 % H_2O

Glass seal:

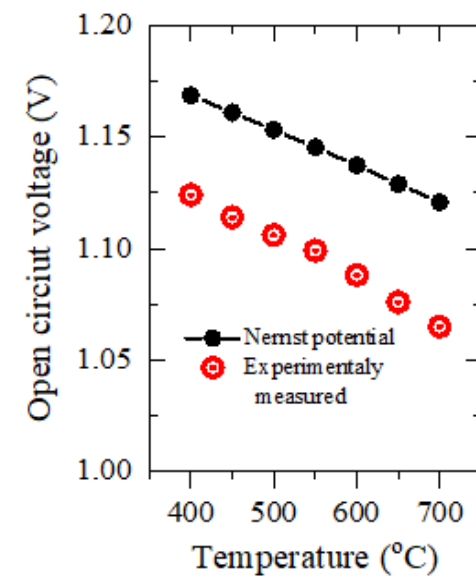
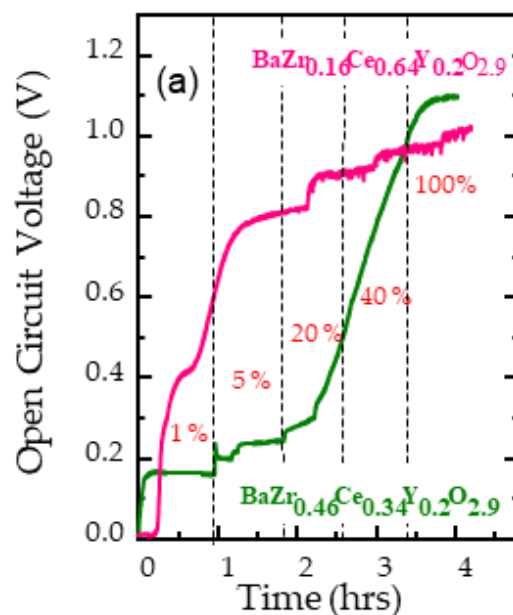
- ✓ Pirex glass
- ✓ 800°C for 1h
- ✓ Reduction @ 600 °C
- ✓ Current collectors
- ✓ O Ag-Pd @ Positrode
- ✓ O Ni mesh @ hydrogen side
- ✓ O Pt #80 mesh at both

Almost no cross leak is observed

- Inlet and outlet flow where very similar (within experimental error)
- No significant leakage through the glass sealant

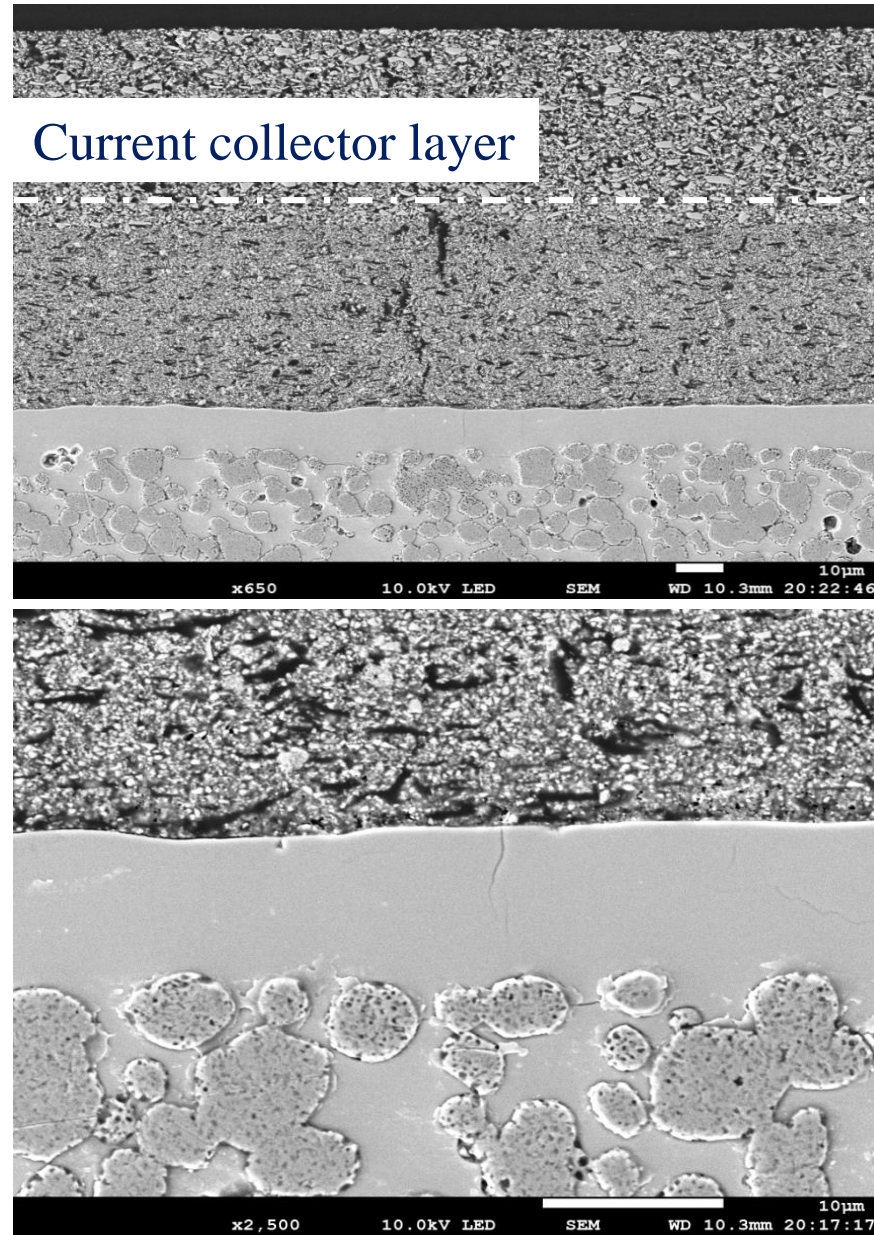
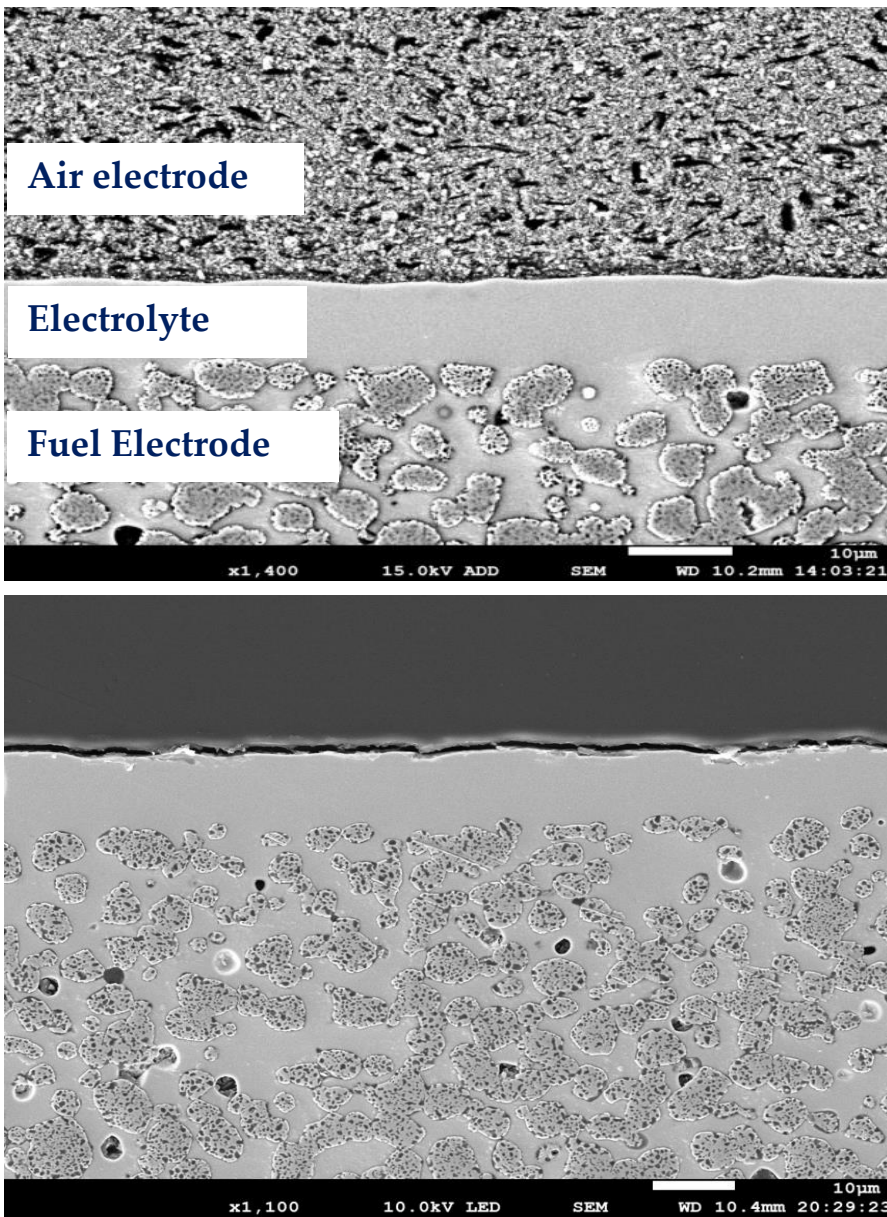


Cell reduction OCV Vs Time and temperature



Typical cell microstructure

Microstructure post measurement

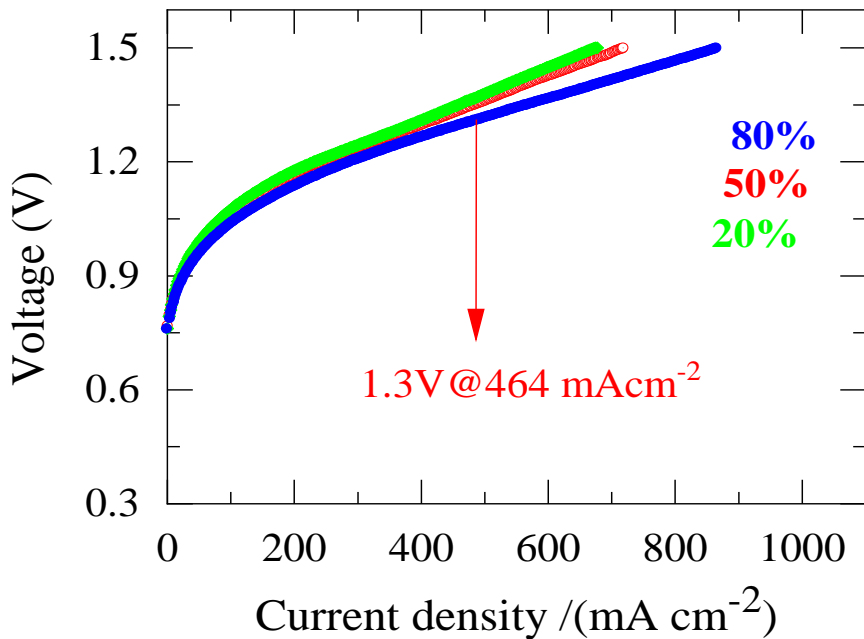


Progress on bottom size cell configuration (PCEC mode)

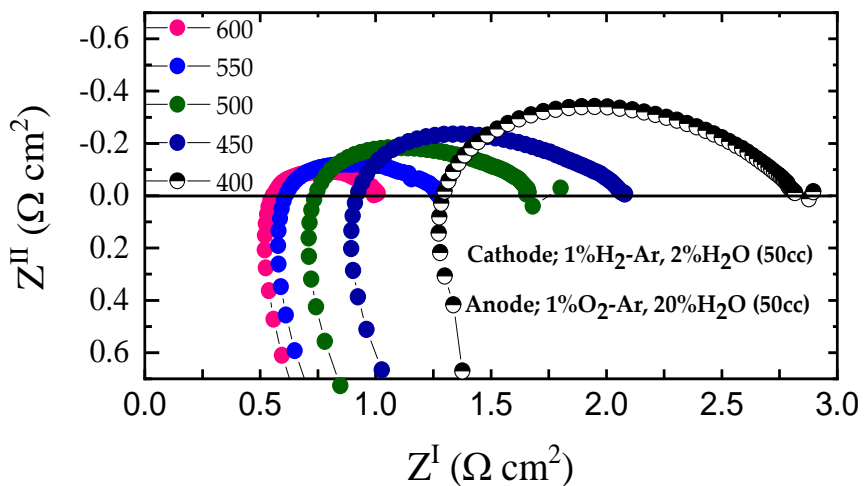
12



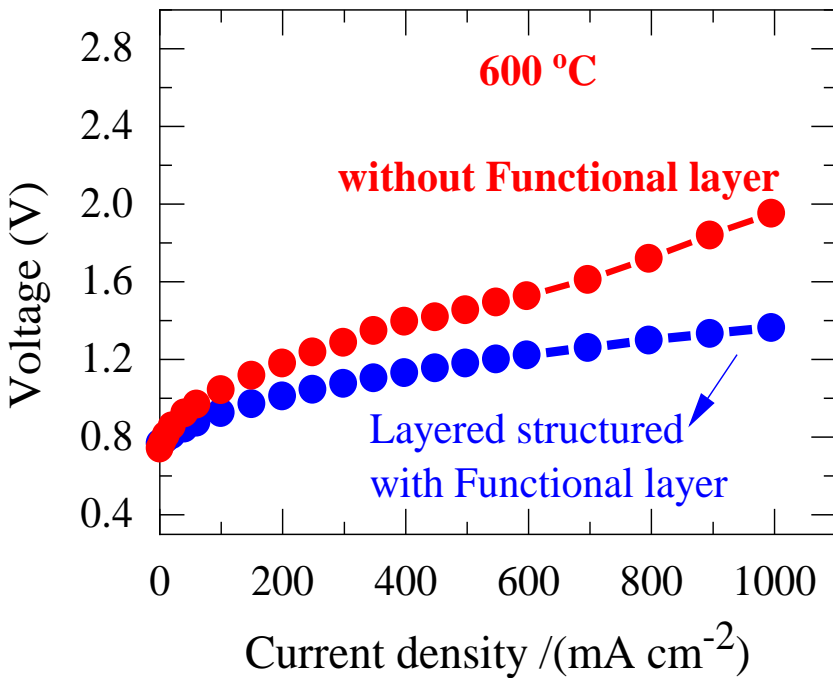
Ba_{0.5}La_{0.5}CoO_{3-δ}|BaZr_{0.44}Ce_{0.36}Y_{0.2}O_{3-δ}



Ba_{0.5}La_{0.5}CoO_{3-δ}|BaZr_{0.16}Ce_{0.64}Y_{0.2}O_{3-δ}



BLC| BZCY| Ni-SZCY541|Ni-BZCY(54)_{8/9}2



Half-cell microstructure

Electrolyte

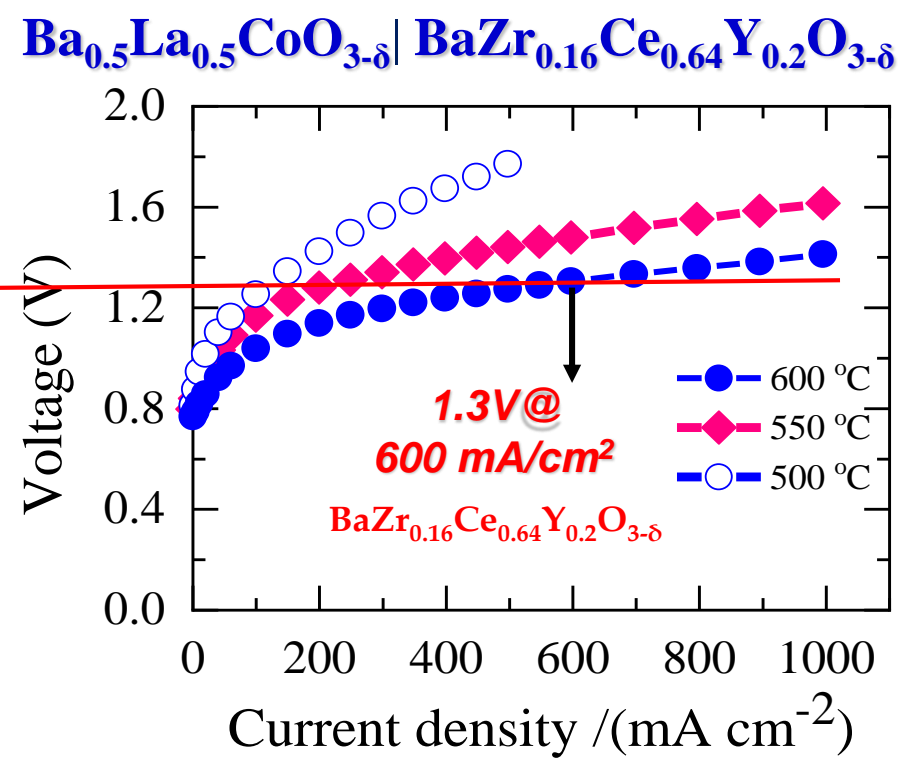
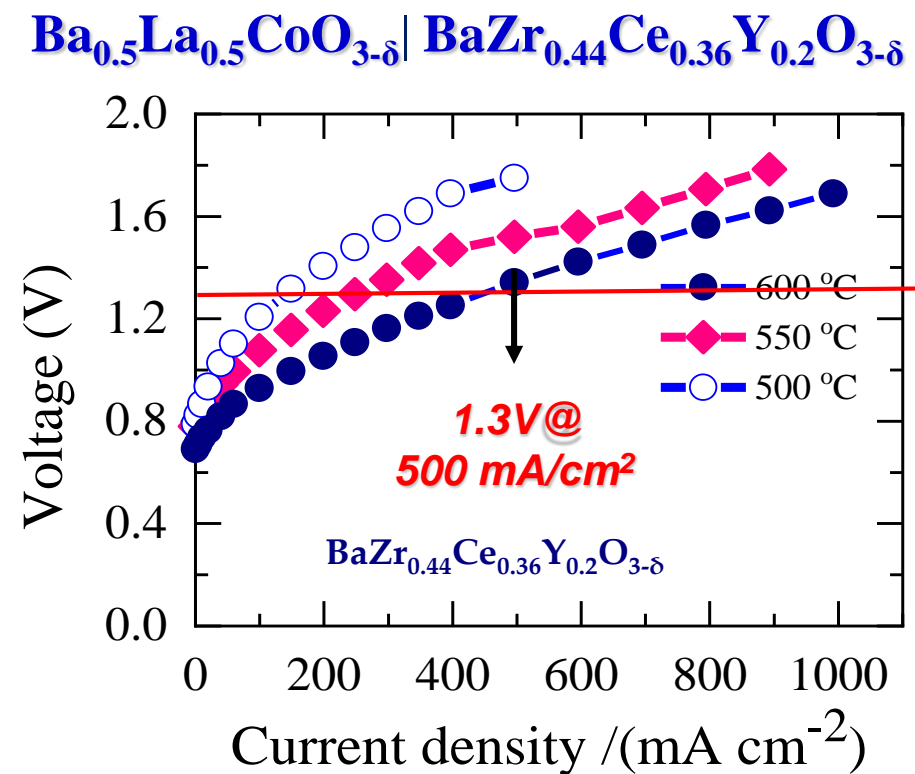
Functional layer

Cathode substrate layer

Steam electrolysis performance (PCEC)

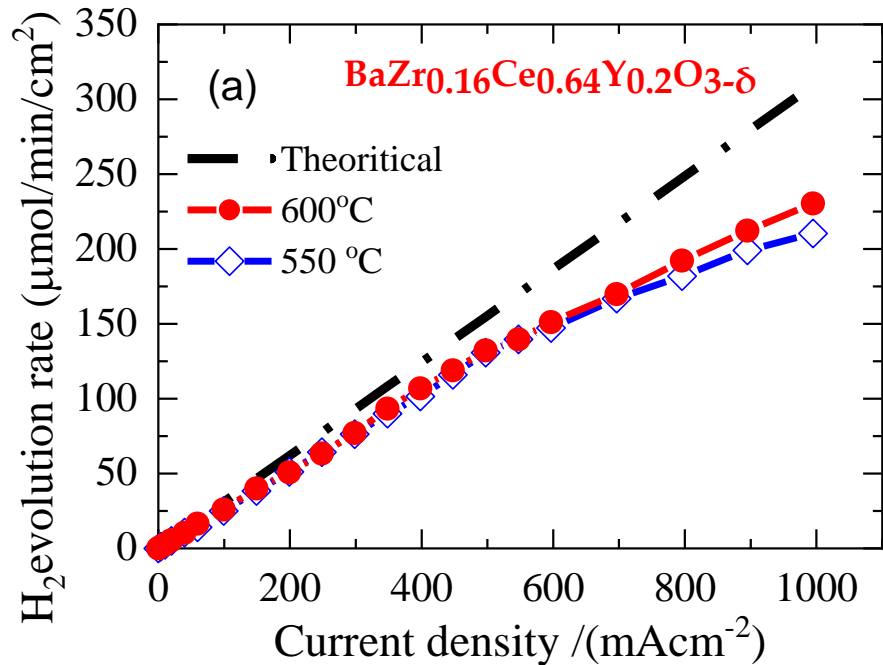
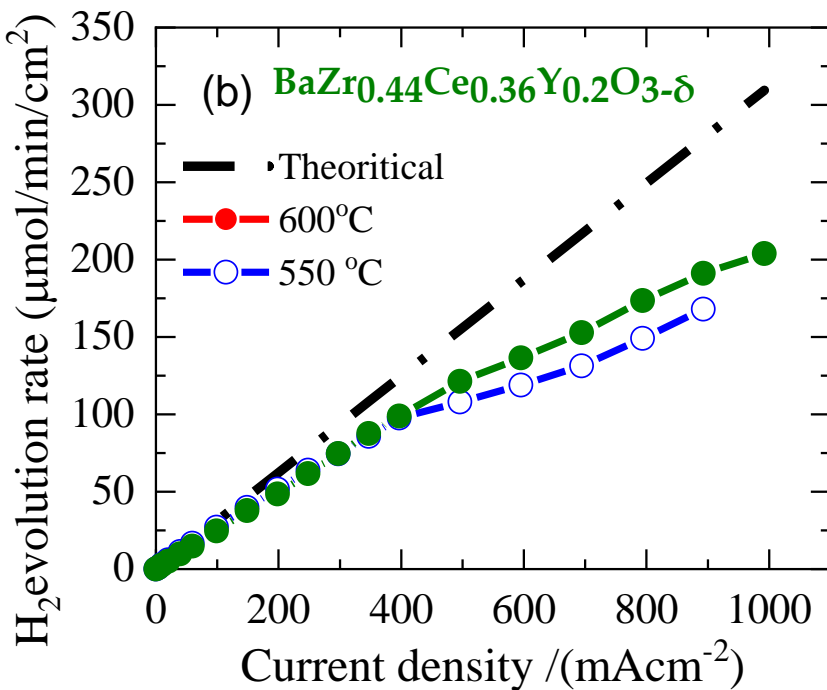
Cell configuration: BLC| BZCY| Ni-SZCY541

I-V characteristics:



Hydrogen evolution rate at 600 and 550 °C

- Hydrogen evolution determined from the increase in hydrogen concentration at the cathode outlet using gas chromatography

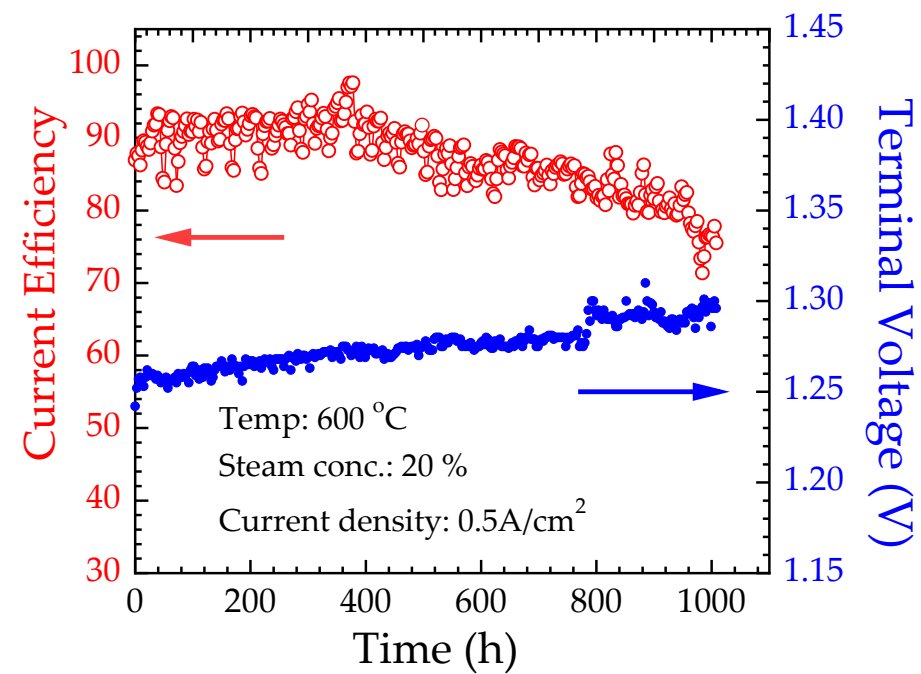


Hydrogen production mirrors Faraday's law
 Deviation at high current density due to
 Electronic leakage
 Current efficiency
 78.5 and 82.7 % at 600°C and 250 mA cm^{-2}

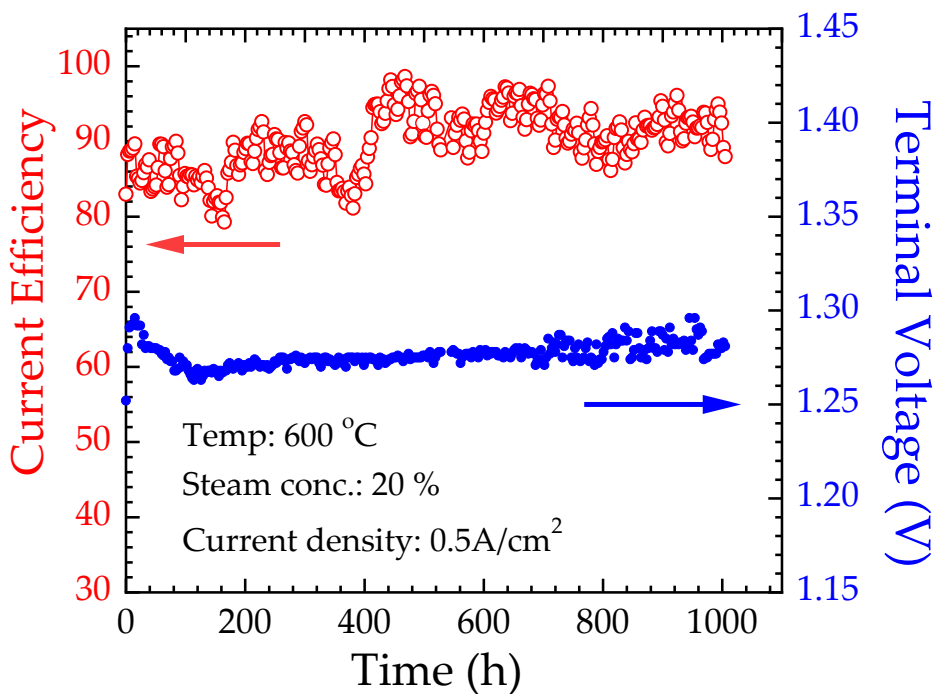
Stable performance
 Current efficiency
 81.5 and 83.1 % at 600°C and 250 mA cm^{-2}
 Impact; The calculated amount of electricity
 to produce 1 Nm^3 of H_2 is 3.8 kWh

Hydrogen Evolution and durability testing

Sample 1 Positrode ($Ba_{0.5}La_{0.5}CoO_3$)



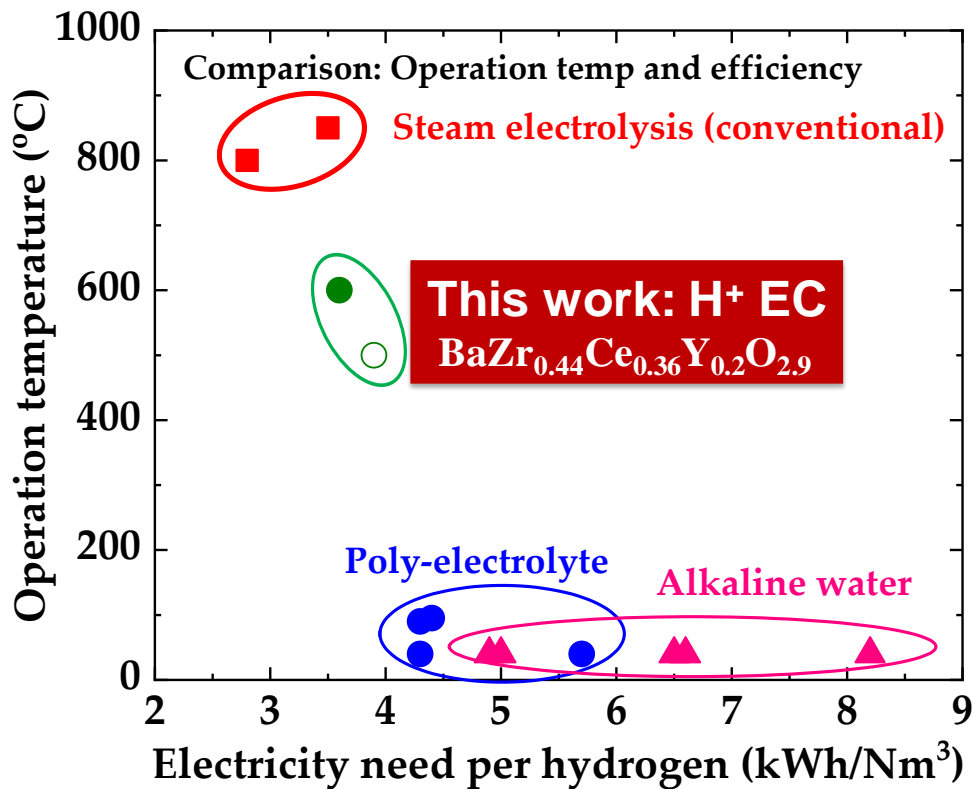
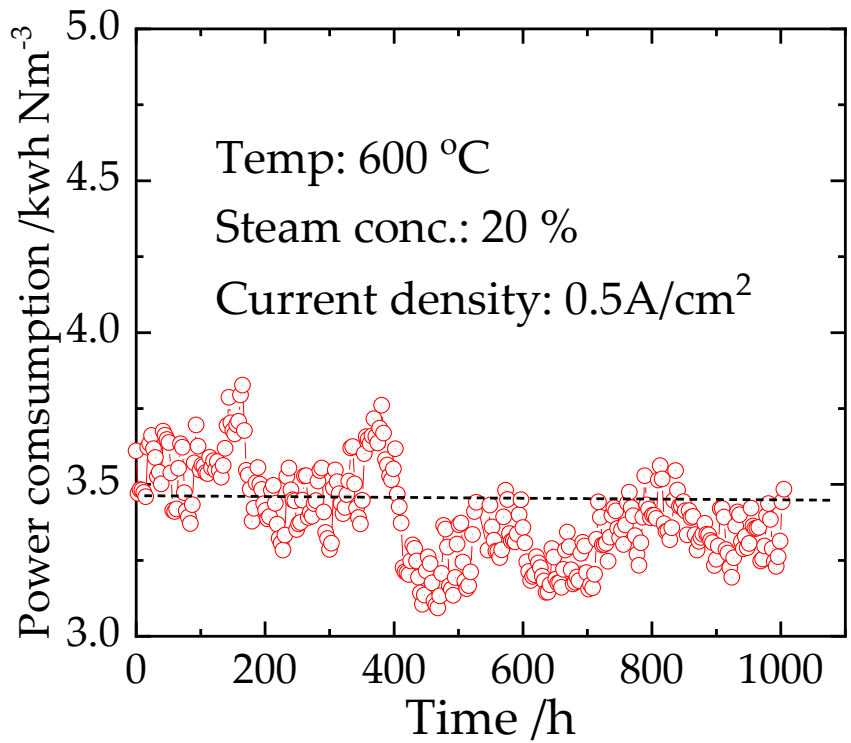
*Sample 2 Positrode ($Ba_{0.5}La_{0.5}CoO_3$)
For reproducibility*



1.25 V@0.5 A/cm², η_{eff} = 80~92% (~10 μ m)

Stable operation, degradation rate < 30mV over 1000 h

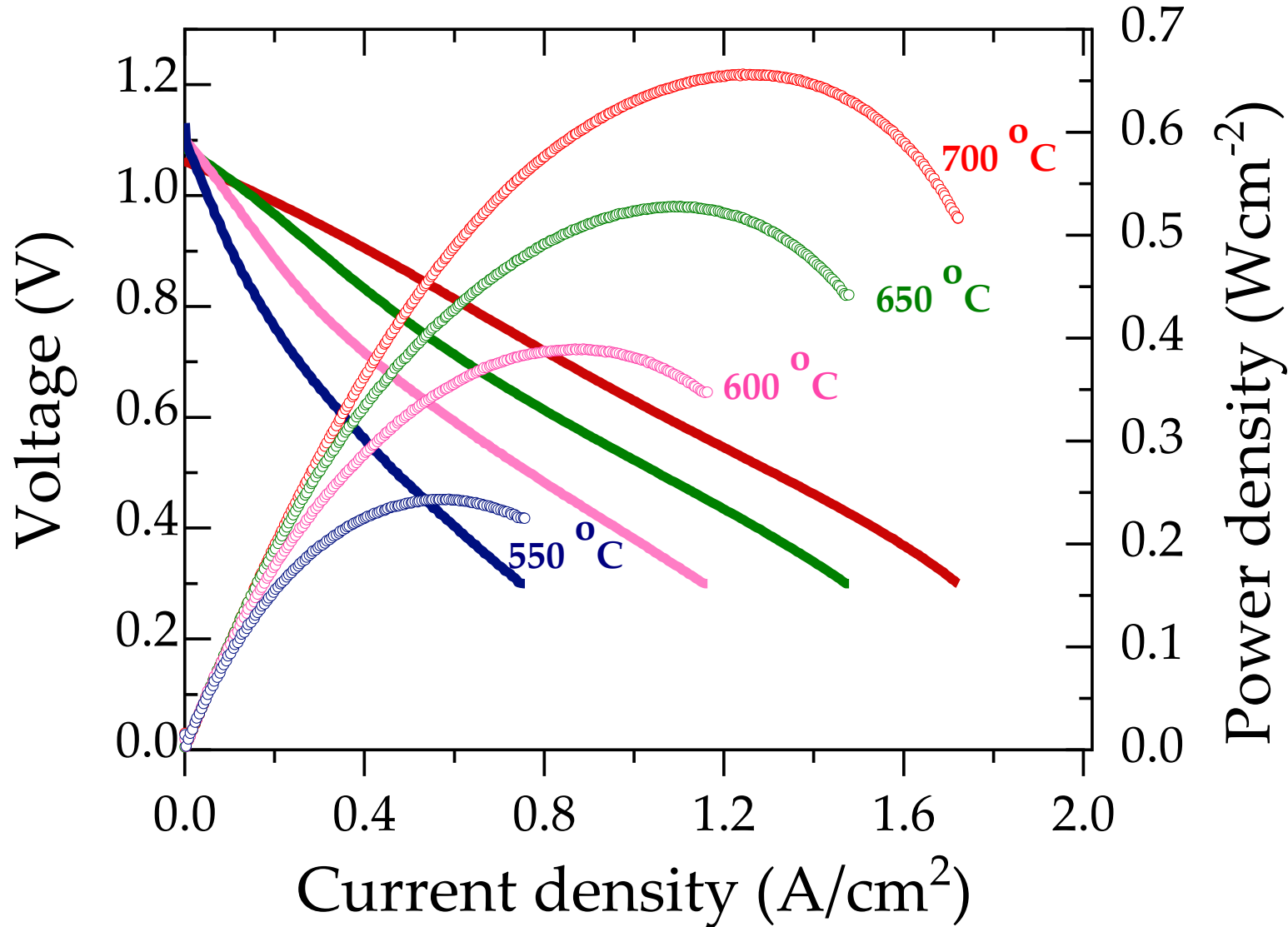
Summary and Comparison



Stable power consumption. Impact; The calculated amount of electricity to produce 1 Nm³ of H₂ is ~3.5 kWh at 600°C

PCFC performance

$\text{Ba}_{0.5}\text{La}_{0.5}\text{CoO}_3$ (BLC55)



- ❖ Deconvolution of physicochemical processes in PCFC, to identify all performance-related polarization processes.

Due to inhomogeneity (Microstructure, gas composition etc.) Electrode processes show different behavior

Distribution function obtained by;

$$Z(\omega) = R_o + Z_{pol}(\omega) = R_o + \int_0^{\infty} \frac{g(t)}{1+j\omega\tau} d\tau$$

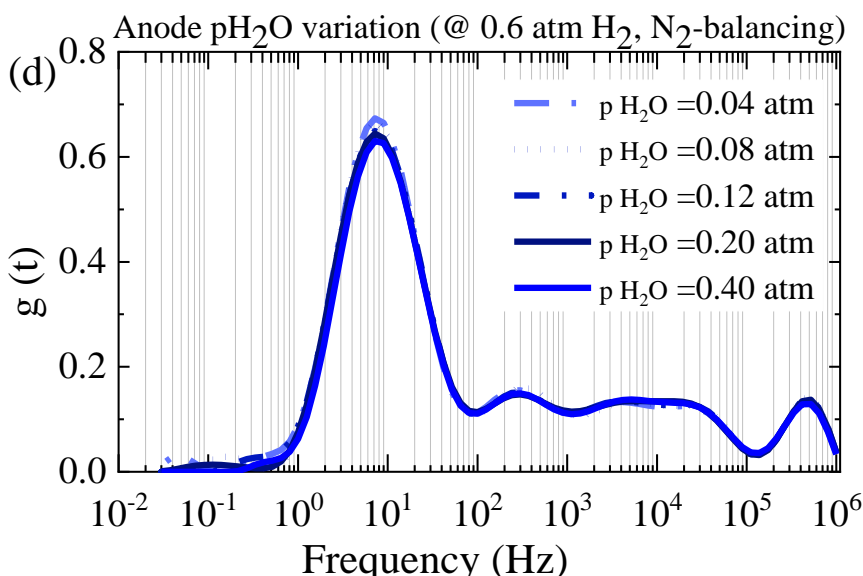
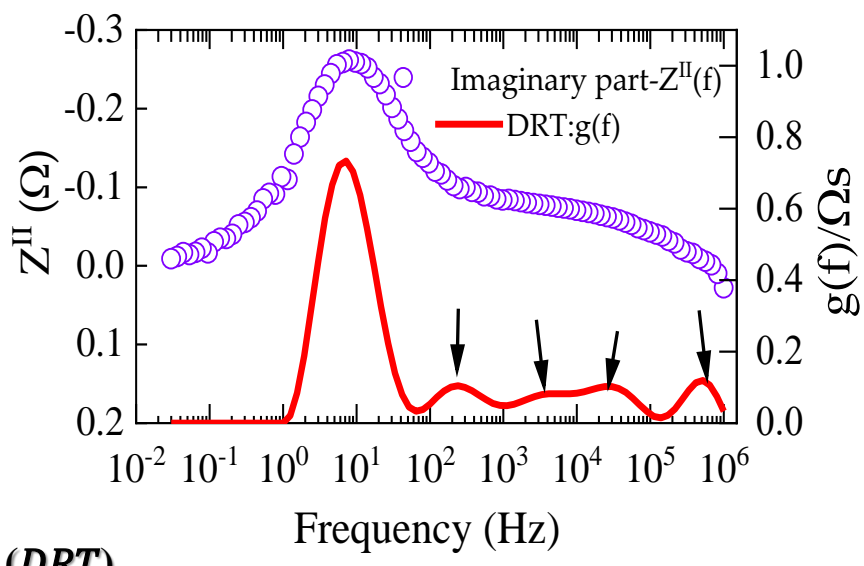
g(f) is the obtained (DRT)

Approach :

- ❖ Stepwise variation of operating Parameters e.g. Temperature Steam partial pressure (pH_2O an) Oxygen partial pressure (pO_2 ,cat)

Results :

- All DRT-peaks are temperature dependent
- Strong impact of the oxidant composition
- The steam content in the fuel shows nearly no effect



Summary

- *$\text{NiO-SrZr}_{0.5}\text{Ce}_{0.4}\text{Y}_{0.1}\text{O}_{3-\delta}$ cathode uniformly promotes densification of $\text{Ba}(\text{Zr}_{0.5}\text{Ce}_{0.4})_{8/9}\text{Y}_{0.2}\text{O}_{2.9}$ at 1350 °C/5h.*



- *The introduction of a $\text{NiO-SrZr}_{0.5}\text{Ce}_{0.4}\text{Y}_{0.1}\text{O}_{3-\delta}$ Functional layer is effective in increasing the triple-phase boundaries and, therefore the cathode activity*



- *Ni diffuse to the electrolyte in the vicinity of NiO grain, resulting in an increase of resistance. High resistance part is in series with the electrode reaction*

Acknowledgements



Prof. Hiroshige Matsumoto
I²CNER Kyushu University



Prof. Tatsumi Ishihara
I²CNER Kyushu University

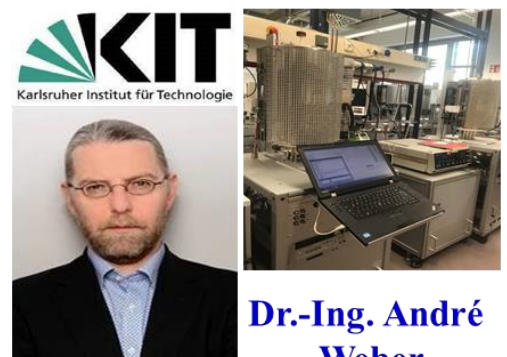
The financial support for this work from the Cross-ministerial Strategic Innovation Promotion Program (SIP), “energy carrier”(Funding agency: JST), JSPS Core-to-Core Program of Advanced Research Networks (Solid Oxide Interfaces for Faster Ion Transport), the Ministry of Economy, Trade and Industry (METI), and by the International Institute for Carbon Neutral Energy Research (I²CNER) sponsored by the World Premier International Research Center Initiative (WPI), MEXT Japan is gratefully acknowledged .



Prof. Wilhelm Albert
Meulenbergh

Dr. Mariya
E. Ivanova

Dr. Wendelin Deibert



**Dr.-Ing. André
Weber**

Thank you for listening